

# Low-Valent Vanadium Complexes of a Pyrrolide-Based Ligand. Electronic Structure of a Dimeric V(II) Complex with a Short and Weak Metal–Metal Bond

Sougandi Ilango,<sup>†</sup> Balamurugan Vidjayacoumar,<sup>†</sup> Sandro Gambarotta,<sup>\*,†</sup> and Serge I. Gorelsky<sup>‡,§</sup>

Department of Chemistry and Laboratory of Computational Chemistry, Centre for Catalysis Research and Innovation, University of Ottawa, Ottawa, Ontario K1N 6N5, Canada

Received November 20, 2007

Deprotonation of the nitrogen atoms of the two pyrrole rings of 1,3-bis-[(1'-pyrrol-2-yl)-1,1'-dimethyl]methyl]benzene with KH followed by further reaction with either  $VCl_3(THF)_3$  or with  $VCl_2(TMEDA)_2$  respectively gave the paramagnetic complexes [1,3-bis-[(1'-pyrrol-2-yl)-1,1'-dimethyl]methyl]benzene]VCl(DME) (**1**) and [1,3-bis-[(1'-pyrrol-2-yl)-1,1'-dimethyl]methyl]benzene]V(THF)<sub>3</sub> (**2**). Further reduction with the appropriate amount of KH afforded diamagnetic dinuclear [1,3-bis-[(1'-pyrrol-2-yl)-1,1'-dimethyl]methyl]benzene]V<sub>2</sub> (**3**). In complex **3**, the bridging interaction between the two metal centers is realized via the ligand central benzene ring. Density functional theory calculations have elucidated the nature of the electronic interaction between the two metals with the bridging  $\pi$ -system thus accounting for its visible structural distortion. Calculations also pointed out the presence of only a weak V–V bond in spite of the short V–V distance.

## Introduction

The low-valent states of vanadium are characterized by very high reactivity which in turn enables a remarkable variety of diversified transformations.<sup>1</sup> At the very basis of the versatility of these derivatives, there is a seemingly general ability to attack the  $\pi$ -system of unsaturated systems<sup>2</sup>

and to act as anchoring agents for metal promoted transformations.<sup>3</sup>

Dinitrogen activation is certainly an important component in the chemistry of the reactivity of low-valent vanadium complexes.<sup>4</sup> The  $d^3$  electron configuration of divalent vanadium makes, in fact, its derivatives particularly suitable for cleaving dinitrogen.<sup>5</sup> This is suggested by the remarkable behavior of  $d^3$  Mo complexes which have marked more than one milestone in dinitrogen activation chemistry.<sup>6</sup> Density functional theory (DFT) calculations have clearly pointed out that the  $\pi$ -coordination of a transient divalent vanadium intermediate to a dinitrogen molecule is at the origin of this remarkable reaction.<sup>5b,c</sup> After almost a decade, these findings still stimulate further research activity<sup>7</sup> for better understanding and hopefully controlling the reactivity of this element with dinitrogen.<sup>8</sup>

The occasional occurrence of metal–metal bonding is another attractive feature also symptomatic of the very high reactivity of low-valent vanadium.<sup>4j,9</sup> The behavior of vanadium with this respect is rather unique and somehow parallels that of divalent chromium. While very short V–V contacts have been observed for bridging ligand systems

\* To whom correspondence should be addressed. E-mail: sgambaro@uottawa.ca.

<sup>†</sup> Department of Chemistry.

<sup>‡</sup> Centre for Catalysis Research and Innovation.

<sup>§</sup> To whom inquiries about DFT calculations should be addressed.

- (1) (a) See, for example, Gambarotta, S.; Jubb, J. In *Comprehensive Organometallic Chemistry*, II ed.; Abel, W. W., Stone, F. G. A., Wilkinson, G., Eds.; Pergamon Press: Oxford, 1995 (and refs. cited therein). (b) Malito, J. *Inorg. Chem.* **2003**, *42*, 149. (c) Toshikazu, H. *Coord. Chem. Rev.* **2003**, *237*, 271. (d) Malito, J. *Inorg. Chem.* **1999**, *38*, 117. (e) Eady, R. R. *Chem. Rev.* **1996**, *96*, 3013. (f) Rehder, D. *Coord. Chem. Rev.* **1999**, *182*, 297. (g) Smith, B. E. *Adv. Inorg. Chem.* **1999**, *47*, 159. (h) Eady, R. R. *Coord. Chem. Rev.* **2003**, *237*, 23. (i) Janas, Z.; Sobota, P. *Coord. Chem. Rev.* **2005**, *249*, 2144.
- (2) (a) See, for example, Jabri, A.; Korobkov, I.; Gambarotta, S.; Duchateau, R. *Angew. Chem., Int. Ed.* **2007**, *46*, 6119. (b) Nowotny, M.; Elschbroich, C.; Behrendt, A.; Massa, W.; Wocadlo, S. *Z. Naturforsch., B* **1993**, *48*, 1581. (c) Ciurli, S.; Floriani, C.; Chiesi-Villa, A.; Guastini, C. *Chem. Commun.* **1986**, 1401. (d) Bolinger, C. M.; Rauchfuss, T. B.; Rheingold, A. L. *J. Am. Chem. Soc.* **1983**, *105*, 6321. (e) Gambarotta, S.; Fiallo, M. L.; Floriani, C.; Chiesi-Villa, A.; Guastini, C. *Inorg. Chem.*, **1984**, *23*, 3532. (f) Gambarotta, S.; Floriani, C.; Chiesi-Villa, A.; Guastini, C. *J. Am. Chem. Soc.* **1983**, *105*, 1690.

- (3) (a) See, for example, Hartung, J.; Ludwig, A.; Demary, M.; Stapf, G. *ACS Symp. Ser.* **2007**, *974*, 38. (Vanadium). (b) Centi, G.; Perathoner, S. *J. Catal.* **1993**, *142*, 84. (c) Gambarotta, S.; Floriani, C.; Chiesi-Villa, A.; Guastini, C. *J. Am. Chem. Soc.* **1982**, *104*, 2019.

capable of accommodating short M–M distances,<sup>9b</sup> unlikely V–V interactions are sufficiently strong to provide the driving force for assembling dimetallic units.<sup>4i,9g</sup> Hence, the attractive possibility, at least in principle, of using the V–V multiple bonds as electron storage units.

As always, the nature of the ligand plays a fundamental role in determining the type of reactivity. Pyrrolyl anion based ligand systems, and especially di and cyclic tetrapyrrolides, have shown a particular versatility in forming clusters and enhancing the chemical reactivity of the metal.<sup>11</sup> The simple pyrrolide anion is per se closely reminiscent of the Cp anion; therefore, a  $\pi$ -bonding mode could primarily be expected. However, both  $\sigma$ - and  $\pi$ -bonding modes are normally recurring,<sup>12</sup> indicating the possibility for the pyrrolide ligand to act as a hemilabile ligand by switching the bonding mode. This characteristic has been recently used

for the design of a vanadium single-component polymerization catalyst.<sup>13</sup> Pyrrolide ligand denticity also plays an important role given that di and polypyrrolides anions at the same time adopt the dual  $\sigma$ - and  $\pi$ -bonding mode, thus favoring the assembly of fairly large cluster structures capable of cooperative multielectron attack on the same substrate.<sup>14</sup> Finally, the observation obtained from lanthanide chemistry that complexes of  $\sigma$ - and  $\pi$ -bonded polypyrrolide anions may indeed enhance the reactivity with respect to the cyclopentadienyl derivative is guiding the search for pyrrole-based ligands, where the  $\pi$ -bonding mode might be constrained not only by the use of Lewis acids<sup>13</sup> but also by the ligand backbone itself.<sup>15</sup>

Following this reasoning, the preparation and characterization of the vanadium derivatives of the tripyrrolide ligand 2,5-{2-[(C<sub>6</sub>H<sub>5</sub>)<sub>2</sub>C]pyrrole}<sub>2</sub>(N-Me-pyrrole) (MeTPH<sub>2</sub>) has recently enabled the preparation and characterization of a divalent vanadium complex, its reaction with dinitrogen, and further reduction toward an unusual nitride bridged mixed valence species.<sup>7</sup> Hence, we have used for this work the 1,3-bis-[1'-pyrrol-2-yl]-1,1'-dimethylmethyl]benzene ligand. We expected that the replacement of the central pyrrolide ring of MeTPH<sub>2</sub> by a phenyl ring would introduce a lower possibility for  $\pi$ -bonding, given the aromaticity of the phenyl ring. Therefore, an even higher reactivity was anticipated.

In this paper, we describe the synthesis and characterization of the V(II) and V(III) complexes of the 1,3-bis-[1'-pyrrol-2-yl]-1,1'-dimethylmethyl]benzene ligand. Since these complexes displayed a surprising inertness toward dinitrogen, further reduction toward even lower oxidation states was then examined. Herein we describe the formation of an unusual diamagnetic, monovalent, vanadium complex with a short V•••V contact.

- (4) (a) Denisov, N. T.; Efimov, O. N.; Shuvalova, N. I.; Shilova, A. K.; Shilov, A. E. *Zh. Fiz. Khim.* **1970**, *44*, 2694.; C.A. **1971**, *74*, 35950. (b) Shilov, A. E.; Denisov, D. N.; Efimov, O. M.; Shuvalov, N. F.; Shuvalova, N. I.; Shilova, A. E. *Nature (London)* **1971**, *231*, 460. (c) Zones, S. I.; Vickery, T. M.; Palmer, J. G.; Schrauzer, G. N. *J. Am. Chem. Soc.* **1976**, *98*, 1289. (d) Zones, S. I.; Palmer, M. R.; Palmer, J. G.; Doemeny, J. G.; Schrauzer, G. N. *J. Am. Chem. Soc.* **1978**, *100*, 2113. (e) Luneva, N. P.; Jarlenski, D. M. L.; Hetherington, D. R. *J. Bacteriol.* **1982**, *150*, 1244. (f) Robson, R. L.; Eady, R. R.; Nikonova, L. A.; Shilov, A. E. *Kinet. Katal.* **1980**, *21*, 1041. (g) Schrauzer, G. N.; Palmer, M. R. *J. Am. Chem. Soc.* **1981**, *103*, 2659. (h) Schrauzer, G. N.; Strampach, N.; Hughes, L. A. *Inorg. Chem.* **1982**, *21*, 2184. (i) Edema, J. J. H.; Meetsma, A.; Gambarotta, S. *J. Am. Chem. Soc.* **1989**, *111*, 6878. (j) Plass, W.; Verkade, J. G. *J. Am. Chem. Soc.* **1992**, *114*, 2275. (k) Rehder, D.; Woitha, C.; Priebisch, W.; Gailus, H. *J. Chem. Soc., Chem. Commun.* **1992**, 364. (l) Ferguson, R.; Solari, E.; Floriani, C.; Chiesi-Villa, A.; Rizzoli, C. *Angew. Chem., Int. Ed. Engl.* **1993**, *32*, 396. (m) Buijink, J. K. F.; Meetsma, A.; Teuben, J. H. *Organometallics* **1993**, *12*, 2004. (n) Berno, P.; Hao, S.; Minhas, R.; Gambarotta, S. *J. Am. Chem. Soc.* **1994**, *116*, 7417. (o) Song, J. -I.; Berno, P.; Gambarotta, S. *J. Am. Chem. Soc.* **1994**, *116*, 6927. (p) Desmangles, N.; Jenkins, H.; Rupp, K. B.; Gambarotta, S. *Inorg. Chim. Acta* **1996**, *250*, 1. (q) Ferguson, R.; Solari, E.; Floriani, C.; Osella, D.; Ravera, M.; Re, N.; Chiesi-Villa, A.; Rizzoli, C. *J. Am. Chem. Soc.* **1997**, *119*, 10104. (r) Shaver, M. P.; Thomson, R. K.; Patrick, B. O.; Fryzuk, M. D. *Can. J. Chem.* **2003**, *81*, 1431. (s) Berno, P.; Gambarotta, S. *Angew. Chem., Int. Ed. Engl.* **1995**, *34*, 822.
- (5) (a) Clentsmith, G. K. B.; Bates, V. M. E.; Hitchcock, P. B.; Cloke, F. G. N. *J. Am. Chem. Soc.* **1999**, *121*, 10444. (b) Bates, V. M. E.; Clentsmith, G. K. B.; Cloke, F. G. N.; Green, J. C.; Jenkin, H. D. L. *Chem. Commun.* **2000**, 927. (c) Studt, F.; Lamarche, V. M. E.; Clentsmith, G. K. B.; Cloke, F. G. N.; Tuzcek, F. *Dalton Trans.* **2005**, 1052.
- (6) (a) Laplaza, C. E.; Cummins, C. C. *Science* **1995**, *268*, 861. (b) Laplaza, C. E.; Johnson, M. J. A.; Peters, J. C.; Odom, A. L.; Kim, E.; Cummins, C. C.; George, G. N.; Pickering, I. J. *J. Am. Chem. Soc.* **1996**, *118*, 8623. (c) Yandulov, D. V.; Schrock, R. R. *J. Am. Chem. Soc.* **2002**, *124*, 6252. (d) Mindiola, D. J.; Meyer, K.; Cherry, J.-P. F.; Baker, T. A.; Cummins, C. C. *Organometallics* **2000**, *19*, 1622. (e) Solari, E.; Da Silva, C.; Iacono, B.; Heschbrouck, J.; Rizzoli, C.; Scopelliti, R.; Floriani, C. *Angew. Chem., Int. Ed.* **2001**, *40*, 3907. (f) Yandulov, D. V.; Schrock, R. R. *Science* **2003**, *301*, 76. (g) Schrock, R. R. *Acc. Chem. Res.* **2005**, *38*, 955.
- (7) (a) Vidyaratne, I.; Gambarotta, S.; Korobkov, I.; Budzelaar, P. H. M. *Inorg. Chem.* **2005**, *44*, 1187. (b) Vidyaratne, I.; Crewdson, P.; Lefebvre, E.; Gambarotta, S. *Inorg. Chem.*, in press.
- (8) Smythe, N. C.; Schrock, R. R.; Muller, P.; Weare, W. W. *Inorg. Chem.* **2006**, *45*, 9197.
- (9) (a) Cotton, F. A.; Daniels, L. M.; Murillo, C. A. *Inorg. Chem.* **1993**, *32*, 2881. (b) Cotton, F. A.; Daniels, L. M.; Murillo, C. A. *Angew. Chem., Int. Ed. Engl.* **1992**, *316*, 737. (c) Cotton, F. A.; Walton, R. A. *Multiple Bonds between Metal Atoms*; J. Wiley and Sons: New York, 1993. (d) Cotton, F. A.; Hillar, E. A.; Murillo, C. A.; Wang, X. *Inorg. Chem.* **2003**, *42*, 6063. (e) Jones, C. J.; O'Hare, D. *Chem. Commun.* **2003**, 2208. (f) Elschembroich, Ch.; Heck, J.; Massa, W.; Nun, E.; Schmidt, R. *J. Am. Chem. Soc.* **1983**, *105*, 2905. (g) Hao, S.; Berno, P.; Minhas, R. K.; Gambarotta, S. *Inorg. Chim. Acta* **1996**, *244*, 37. (10) Edema, J. J. H.; Gambarotta, S. *Comments Inorg. Chem.* **1991**, *4*, 195.
- (11) (a) Jubb, J.; Gambarotta, S. *J. Am. Chem. Soc.* **1994**, *116*, 4477. (b) Dube, T.; Conoci, S.; Gambarotta, S.; Yap, G. P. A.; Vasapollo, G. *Angew. Chem., Int. Ed.* **1999**, *38*, 3657. (c) Guan, J.; Dube, T.; Gambarotta, S.; Yap, G. P. A. *Organometallics* **2000**, *19*, 4820. (d) Dube, T.; Ganesan, M.; Conoci, S.; Gambarotta, S.; Yap, G. P. A. *Organometallics*, **2000**, *19*, 3716. (e) Korobkov, I.; Gambarotta, S.; Yap, G. P. A. *Angew. Chem., Int. Ed.* **2002**, *41*, 3433. (f) Ganesan, M.; Lalonde, M. P.; Gambarotta, S.; Yap, G. P. A. *Organometallics* **2001**, *20*, 2443. (g) Ganesan, M.; Berube, C. D.; Gambarotta, S.; Yap, G. P. A. *Organometallics* **2002**, *21*, 1707. (h) Freckmann, D. M. M.; Dube, T.; Berube, C. D.; Gambarotta, S.; Yap, G. P. A. *Organometallics* **2002**, *21*, 1240. (i) Berube, C. D.; Gambarotta, S.; Yap, G. P. A. *Organometallics* **2003**, *22*, 3742. (j) Crewdson, P.; Gambarotta, S.; Yap, G. P. A.; Thompson, L. K. *Inorg. Chem.* **2003**, *42*, 8579.
- (12) (a) For a few selected examples, see Coucouvanis, D.; Salifoglou, A.; Kanatzidis, M. G.; Simopoulos, A.; Papaefthymiou, V. *J. Am. Chem. Soc.* **1984**, *106*, 6081. (b) Driver, M. S.; Hartwig, J. F. *Organometallics* **1998**, *17*, 1134. (c) Lee, H.; Bonanno, J. B.; Hascall, T.; Cordaro, J.; Hahn, J. M.; Parkin, G. *J. Chem. Soc., Dalton Trans.* **1999**, 1365. (d) Novak, A.; Blake, A. J.; Wilson, C.; Love, J. B. *Chem. Commun.* **2002**, 2796. (e) Scott, J.; Gambarotta, S.; Yap, G. P. A.; Rancourt, D. G. *Organometallics* **2003**, *22*, 2325. (f) Salo, E. V.; Guan, Z. *Organometallics* **2003**, *22*, 5033. (g) Hock, A. S.; Schrock, R. R.; Hoveyda, A. H. *J. Am. Chem. Soc.* **2006**, *128*, 16373.
- (13) Jabri, A.; Korobkov, I.; Gambarotta, S.; Duchateau, R. *Angew. Chem., Int. Ed.* **2007**, *46*, 6119.
- (14) (a) See, for example, Ganesan, M.; Gambarotta, S.; Yap, G. P. A. *Angew. Chem., Int. Ed.* **2001**, *40*, 766.
- (15) Arunachalampillai, A.; Crewdson, P.; Korobkov, I.; Gambarotta, S. *Organometallics* **2006**, *25*, 3856.

## Experimental Section

All operations were performed under an atmosphere of dry, oxygen-free purified nitrogen employing both standard Schlenk line techniques and a Vacuum Atmospheres inert atmosphere glovebox. Solvents were dried by using an aluminum oxide solvent purification system. Centrifugations and decantations, as well as sample preparation, were carried out inside the glovebox. The ligand 1,3-bis-[(1'-pyrrol-2-yl)-1,1'-dimethyl methyl]benzene<sup>16</sup> was synthesized according to literature procedure. The starting materials V<sup>II</sup>Cl<sub>2</sub>(TMEDA)<sub>2</sub><sup>17</sup> and V<sup>III</sup>Cl<sub>3</sub>(THF)<sub>3</sub><sup>18</sup> were synthesized according to the reported literature procedures. NMR spectra were recorded on a Bruker Avance 300 spectrometer. Infrared spectra were recorded on a ABB Bomen FT-IR instrument from Nujol mulls prepared in the glovebox. Elemental analyses were performed on a Perkin-Elmer 2400 CHN analyzer. Data for X-ray crystal structure determinations were obtained with a Bruker diffractometer equipped with a 1K Smart CCD area detector at 200K.

**Preparation of [1,3-bis-[(1'-pyrrol-2-yl)-1,1'-dimethyl]methyl]benzene[VCl(DME)] (1).** A solution of 1,3-bis-[(1'-pyrrol-2-yl)-1,1'-dimethyl]methyl]benzene (0.292 g, 1.0 mmol) in THF (10 mL) was treated with KH (0.088 g, 2.2 mmol) and stirred overnight to give a light yellow solution. Addition of VCl<sub>3</sub>(THF)<sub>3</sub> (0.373 g, 1.0 mmol) to the above solution changed the color to dark green. Stirring was continued for an additional 6 h. The solvent was completely removed in vacuum, and the residue was redissolved in DME (5 mL). The mixture was then centrifuged to discard the insoluble colorless white solid, and the centrifugate was reduced to half of its original volume to yield X-ray quality green crystals of **1** (0.350 g, 0.78 mmol, 78%) after two days at room temperature. Anal. Calcd (found) for C<sub>24</sub>H<sub>32</sub>N<sub>2</sub>O<sub>2</sub>ClV: C, 61.68 (61.59); H, 6.85 (6.32); N, 5.99 (5.78).  $\mu_{\text{eff}} = 2.76 \mu_{\text{B}}$ .

**Preparation of [1,3-bis-[(1'-pyrrol-2-yl)-1,1'-dimethyl]methyl]benzene[V(THF)<sub>3</sub>] (2).** A solution of 1,3-bis-[(1'-pyrrol-2-yl)-1,1'-dimethyl]methyl]benzene (0.292 g, 1.0 mmol) in THF (10 mL) was treated with KH (0.088 g, 2.2 mmol) and stirred overnight to give a light yellow solution. Addition of VCl<sub>2</sub>(TMEDA)<sub>2</sub> (0.354 g, 1.0 mmol) to the above solution changed the color to dark green. The stirring was continued for an additional 6 h. The solvent was completely removed in vacuum, and the residue was redissolved in THF (5 mL). The mixture was then centrifuged to discard the insoluble solid, and the centrifugate was layered with *n*-hexanes to yield X-ray quality dark green crystals of **2** (0.330 g, 0.59 mmol, 59%) Anal. Calcd (found) for C<sub>32</sub>H<sub>46</sub>N<sub>2</sub>O<sub>3</sub>V: C, 68.86 (67.59); H, 8.25 (8.32); N, 5.02 (4.78).  $\mu_{\text{eff}} = 3.55 \mu_{\text{B}}$ .

**Preparation of [(THF)<sub>2</sub>K(1,3-bis-[(1'-pyrrol-2-yl)-1,1'-dimethyl]methyl]benzene)V<sup>I</sup>]<sub>2</sub>] (3).** **Method A.** A solution of **1** (0.467 g, 0.50 mmol) in THF (10 mL) was treated with KH (0.088 g, 2.2 mmol) and stirred over a period of 1 week. The green color solution changed to a dark solution. The solvent was completely removed in vacuum, and the residue was redissolved in THF (5 mL). The mixture was then centrifuged to discard the insoluble solid, and the centrifugate was layered with *n*-hexanes to yield X-ray quality dark brown crystals of **3** (0.120 g, 0.23 mmol, 22%) after 2 days at room temperature.

**Method B.** A solution of **2** (0.557 g, 0.50 mmol) in THF (10 mL) was treated with KH (0.044 g, 1.1 mmol) and stirred over a period of one week. The green color solution changed to dark

colored solution. The solvent was completely removed in vacuum, and the residue was redissolved in THF (5 mL). The mixture was then centrifuged to eliminate a small amount of insoluble solid, and the centrifugate was layered with *n*-hexanes to yield X-ray quality dark brown crystals of **3** (0.086 g, 0.164 mmol, 16%) after 2 days at room temperature.

**Method C.** A solution of 1,3-bis-[(1'-pyrrol-2-yl)-1,1'-dimethyl]methyl]benzene (0.29 g, 1.0 mmol) in THF (10 mL) was treated with KH (0.12 g, 3.1 mmol) and stirred overnight to give a light yellow solution. Addition of VCl<sub>2</sub>(TMEDA)<sub>2</sub> (0.354 g, 1.0 mmol) to the above solution formed a dark brown solution. After continued stirring overnight, the solvent was completely removed in vacuum, and the residue was redissolved in THF (5 mL). The mixture was then centrifuged to discard a small amount of insoluble solid, and the centrifugate was layered with *n*-hexanes to yield X-ray quality dark brown crystals of **3** (0.62 g, 0.59 mmol, 40%) after 2 days at room temperature.

**Method D.** A solution of 1,3-bis-[(1'-pyrrol-2-yl)-1,1'-dimethyl]methyl]benzene (0.29 g, 1.0 mmol) in THF (10 mL) was treated with KH (0.164 g, 4.1 mmol) and stirred overnight to give a light yellow solution. Addition of V<sup>III</sup>Cl<sub>3</sub>(THF)<sub>3</sub> (0.373 g, 1.0 mmol) to the above solution changed the color to dark brown. Stirring was continued overnight after which the solvent was completely removed in vacuum. The residue was redissolved in THF (5 mL), the resulting mixture was then centrifuged to discard the insoluble colorless solid, and the centrifugate was layered with *n*-hexanes to yield X-ray quality dark brown crystals of **3** (0.360 g, 0.344 mmol, 24%). Anal. Calcd (found) for C<sub>56</sub>H<sub>76</sub>N<sub>4</sub>O<sub>4</sub>K<sub>2</sub>V<sub>2</sub>: C, 64.12 (63.59); H, 6.81 (6.62); N, 5.34 (5.28). <sup>1</sup>H NMR (25 °C, THF-*d*<sub>6</sub>, 500 MHz):  $\delta$  9.47 (s, aromatic, 1H), 7.25–6.89 (m, aromatic, 3H), 6.54 (s, pyrrole, 2H), 5.91 (d, pyrrole, 4H), 3.59 (d, THF, 8H), 1.75 (d, THF, 8H), 1.56 (s, Me, 12H). <sup>13</sup>C NMR (25 °C, THF-*d*<sub>6</sub>, 125.7 MHz): 150.69 (quat. Ph), 140.48 (quat. Pyrr), 129.71, 126.09, 124.52 (C–H, Ph), 117.42, 107.41, 104.99 (C–H pyrr), 40.18 [quat. C(Me)<sub>2</sub>], 30.67 (Me), 68.32, 68.21, 26.98, 26.89 (THF).

**DFT Calculations.** All calculations were performed using the Gaussian 03 package.<sup>19</sup> Stationary points on the potential energy surface were obtained using the B3LYP<sup>20,21</sup> and PBE<sup>22,23</sup> exchange-correlation functionals. The TZVP<sup>24</sup> basis set for all atoms was used for all calculations except for complex **3** for which the

(16) Sessler, J. L.; Cho, W.-S.; Lynch, V.; Král, V. *Chem.—Eur. J.* **2002**, *8*, 1134.  
 (17) Edema, J. J. H.; Stauthamer, W.; Gambarotta, S.; Van-Bolhuis, F.; Spek, A. L. *Inorg. Chem.* **1990**, *29*, 2147.  
 (18) Manzer, L. E. *Inorg. Synth.* **1982**, *21*, 138.

(19) Frisch, M. J.; Trucks, G. W.; Schlegel, H. B.; Scuseria, G. E.; Robb, M. A.; Cheeseman, J. R.; Montgomery, J. J. A.; Vreven, T.; Kudin, K. N.; Burant, J. C.; Millam, J. M.; Lyengar, S. S.; Tomasi, J.; Barone, V.; Mennucci, B.; Cossi, M.; Scalmani, G.; Rega, N.; Petersson, G. A.; Nakatsuji, H.; Hada, M.; Ehara, M.; Toyota, K.; Fukuda, R.; Hasegawa, J.; Ishida, M.; Nakajima, T.; Honda, Y.; Kitao, O.; Nakai, H.; Klene, M.; Li, X.; Knox, J. E.; Hratchian, H. P.; Cross, J. B.; Adamo, C.; Jaramillo, J.; Gomperts, R.; Stratmann, R. E.; Yazyev, O.; Austin, A. J.; Cammi, R.; Pomelli, C.; Ochterski, J. W.; Ayala, P. Y.; Morokuma, K.; Voth, G. A.; Salvador, P.; Dannenberg, J. J.; Zakrzewski, V. G.; Dapprich, S.; Daniels, A. D.; Strain, M. C.; Farkas, O.; Malick, D. K.; Rabuck, A. D.; Raghavachari, K.; Foresman, J. B.; Ortiz, J. V.; Cui, Q.; Baboul, A. G.; Clifford, S.; Cioslowski, J.; Stefanov, B. B.; Liu, G.; Liashenko, A.; Piskorz, P.; Komaromi, I.; Martin, R. L.; Fox, D. J.; Keith, T.; Al-Laham, M. A.; Peng, C. Y.; Nanayakkara, A.; Challacombe, M.; Gill, P. M. W.; Johnson, B.; Chen, W.; Wong, M. W.; Gonzalez, C.; Pople, J. A. *Gaussian 03*, revision C.01; Gaussian, Inc.: 2003.  
 (20) Becke, A. D. *J. Chem. Phys.* **1993**, *98*, 5648.  
 (21) Lee, C.; Yang, W.; Parr, R. G. *Phys. Rev.* **1988**, *B37*, 785.  
 (22) Perdew, J. P.; Burke, K.; Ernzerhof, M. *Phys. Rev. Lett.* **1996**, *77*, 3865.  
 (23) Perdew, J. P.; Burke, K.; Ernzerhof, M. *Phys. Rev. Lett.* **1997**, *78*, 1396.  
 (24) Schafer, A.; Huber, C.; Ahlrichs, R. *J. Chem. Phys.* **1994**, *100*, 5829.



**Table 1.** Crystal Data and Structure Refinement Data for **1**, **2**, and **3**

complex	<b>1</b>	<b>2</b>	<b>3</b>
empirical formula	C <sub>24</sub> H <sub>32</sub> N <sub>2</sub> O <sub>2</sub> ClV	C <sub>32</sub> H <sub>46</sub> N <sub>2</sub> O <sub>3</sub> V	C <sub>28</sub> H <sub>38</sub> N <sub>2</sub> O <sub>2</sub> KV
mol wt	466.91	557.65	524.64
cryst syst	monoclinic	monoclinic	monoclinic
space group, Z	P2 <sub>1</sub> /c, 4	P2 <sub>1</sub> , 4	P2 <sub>1</sub> /c, 4
a (Å)	11.256(2)	10.575(5)	10.777(4)
b (Å)	15.450(3)	12.891(7)	10.249(4)
c (Å)	14.891(4)	11.341(6)	23.712(10)
α (°)	90.0	90.0	90.0
β (°)	116.198(3)	110.400(9)	90.844(7)
γ (°)	90.0	90.0	90.0
V (Å <sup>3</sup> )	2323.7(9)	1449.0(13)	2618.8(18)
ρ <sub>calcd</sub> (g cm <sup>-3</sup> )	1.335	1.278	1.331
μ <sub>calcd</sub> (mm <sup>-1</sup> )	0.564	0.377	0.565
F <sub>000</sub>	984	598	1112
No. of total reflns	17 064	10 504	13 492
No. of unique reflns	3929	4881	3156
R(int)	0.0428	0.0354	0.0939
GOF	1.018	1.003	1.034
R <sub>1</sub> , wR <sub>2</sub> (I > 2σ(I)) <sup>a</sup>	0.0429, 0.1016	0.0398, 0.0888	0.0541, 0.1245
R <sub>1</sub> , wR <sub>2</sub> (all data) <sup>a</sup>	0.0641, 0.1122	0.0529, 0.0943	0.0944, 0.1437
max/min electron density (e <sup>-</sup> Å <sup>-3</sup> )	0.379 and -0.380	0.370 and -0.172	0.695 and -0.270

$$^a R(F) = \frac{\sum(|F_o| - |F_c|)}{\sum|F_o|}; R_w(F^2) = \frac{\sum[w(|F_o|^2 - |F_c|^2)]}{\sum[w(|F_o|^2)]}^{1/2}.$$

DGDZVP<sup>25</sup> basis set was used (because of the large number of atoms in the complex). Tight self-consistent field convergence criteria were used for all calculations. The converged wave functions were tested to confirm that they corresponded to the ground-state surface. The second-order derivative of the energy with respect to nuclear positions was evaluated to determine the nature of the stationary points. Vibrational zero point energies (ZPE) and thermal corrections were included in the calculation of the free energies at 298 K and 1 atm.

Atomic charges were calculated by the natural population analysis (NPA)<sup>26</sup> as implemented in Gaussian 03. Two- and three-center bond orders and valence indexes (V) were obtained using the AOMix-L program.<sup>27–29</sup> Charge decomposition analysis, analysis of molecular orbitals in terms of fragment orbital (FO) contributions, and construction of the FO interaction diagrams were carried out using the AOMix-CDA program.<sup>30,31</sup>

**X-ray Crystallography.** Suitable single crystals of **1**, **2**, and **3** were carefully selected under the microscope, mounted on a thin, glass fiber with paraffin oil, and cooled to the data collection temperature. X-ray data were collected on a Bruker AXS SMART 1k CCD diffractometer at 200(2) K equipped with graphite-monochromated Mo Kα radiation (λ = 0.71073 Å). Initial unit-cell parameters were determined from 60 data frames collected at different sections of the Ewald sphere. The intensity data were corrected for Lorentz and polarization effects; the empirical absorption correction (SADABS) was applied.<sup>32</sup> The structures were solved by direct methods, completed with successive difference Fourier syntheses, and refined by full-matrix least-squares methods based on F<sup>2</sup> using SHELXL-97. All nonhydrogen atoms were refined anisotropically, and all the hydrogen atoms were fixed

geometrically and were not refined. All scattering factors and anomalous dispersion factors are contained in the SHELXTL 6.12 program.<sup>33</sup> A summary of the data collection and structure refinement information is provided in Table 1 while pertinent bond distances and bond angles are tabulated in Table 2.

## Results and Discussion

The deprotonation of 1,3-bis-[[1-(1'-pyrrol-2-yl)-1,1'-dimethyl]methyl]benzene was conveniently carried out in situ with two equivalents of KH in THF. Subsequent reaction with either VCl<sub>3</sub>(THF)<sub>3</sub> or VCl<sub>2</sub>(TMEDA)<sub>2</sub> gave the corresponding paramagnetic complexes [1,3-bis-[[1-(1'-pyrrol-2-yl)-1,1'-dimethyl]methyl]benzene]VCl(DME) (**1**) and [1,3-bis-[[1-(1'-pyrrol-2-yl)-1,1'-dimethyl]methyl]benzene]V(THF)<sub>3</sub> (**2**) after crystallization from the appropriate solvent (Scheme 1). In both cases the crystallinity was sufficient to undertake X-ray crystal structure determinations. Both complexes display solid state magnetic moments as expected for the high spin d<sup>2</sup> and d<sup>3</sup> configuration of the tri and divalent vanadium, respectively.

The crystal structure of **1** (Figure 1) consists of a trivalent vanadium center in a distorted octahedral environment defined by two oxygen donor atoms [V–O = 2.151 Å; O–V–O = 75.2°] of the DME ligand, one chlorine [V–Cl = 2.361 Å], and two nitrogen atoms [V–N = 1.986 Å] of the two deprotonated pyrrole rings. The two DME oxygen atoms and the two nitrogen donors define the equatorial plane [O–V–N = 88.3°/163.2°]. The chlorine ligand is located on the axial position trans to the phenyl ring. The orientation of the central phenyl ring is closely reminiscent of π-bonding. However, all the V–C distances are beyond the normal bonding range with the exception of the C contained between the two attachments which can be considered as at the limit of the V–C bonding range [2.517(3) Å]. The tilting of the phenyl ring [103.6°], as well as its undisturbed planarity, rules out the idea that the ring might have been deprotonated.

(25) Godbout, N.; Salahub, D. R.; Andzelm, J.; Wimmer, E. *Can. J. Chem.* **1992**, *70*, 560.

(26) Reed, A. E.; Curtiss, L. A.; Weinhold, F. *Chem. Rev.* **1988**, *88*, 899.

(27) Mayer, I. *Chem. Phys. Lett.* **1983**, *97*, 270.

(28) Sannigrahi, A. B.; Kar, T. *Chem. Phys. Lett.* **1990**, *173*, 569.

(29) Gorelsky, S. I.; Basumallick, L.; Vura-Weis, J.; Sarangi, R.; Hedman, B.; Hodgson, K. O.; Fujisawa, K.; Solomon, E. I. *Inorg. Chem.* **2005**, *44*, 4947.

(30) Gorelsky, S. I. *AOMix: Program for Molecular Orbital Analysis*, version 6.36; University of Ottawa: Ottawa, Canada, 2007.

(31) Gorelsky, S. I.; Ghosh, S.; Solomon, E. I. *J. Am. Chem. Soc.* **2006**, *128*, 278.

(32) Blessing, R. *Acta Crystallogr.* **1995**, *A51*, 33.

(33) Sheldrick, G. M.; Bruker AXS: Madison, WI, 2001.

**Table 2.** Pertinent Bond Distances (Å) and Bond Angles (deg) for **1**, **2**, and **3**

complex <sup>a</sup>	1	2	3
V(1)–N(1)	1.992(2)	2.143(2)	2.148(4)
V(1)–N(2)	1.980(2)	2.165(2)	2.152(4)
V(1)–O(1)	2.135(2)	2.200(2)	
V(1)–O(2)	2.167(2)	2.168(2)	
V(1)–O(3)		2.174(2)	
V(1)–Cl(1)	2.361(1)		
V(1)–C(13)	2.517(3)	2.615(1)	
V(1)–cent(1)			1.916(2)
V(1)–cent(2)			2.065(3)
V(1)···V(1')			2.412(1)
K(1)–O(1)			2.705(5)
K(1)–O(2)			2.653(5)
K(1)–cent(3)			2.862(9)
K(1)–cent(4)			2.859(8)
N(1)–V(1)–N(2)	106.6(1)	176.1(1)	91.2(2)
N(1)–V(1)–O(1)	88.3(1)	88.7(1)	
N(1)–V(1)–O(2)	163.2(1)	90.0(1)	
N(1)–V(1)–O(3)		93.0(1)	
N(1)–V(1)–Cl(1)	96.1(1)		
N(1)–V(1)–C(13)	79.8(1)	87.0(1)	
N(1)–V(1)–cent(1)			106.9(1)
N(1)–V(1)–cent(2)			96.5(1)
N(2)–V(1)–O(1)	164.4(1)	90.5(1)	
N(2)–V(1)–O(2)	89.6(1)	91.2(1)	
N(2)–V(1)–O(3)		90.8(1)	
N(2)–V(1)–Cl(1)	95.3(1)		
N(2)–V(1)–C(13)	79.9(1)	89.2(1)	
N(2)–V(1)–cent(1)			106.5(1)
N(2)–V(1)–cent(2)			97.1(1)
O(1)–V(1)–O(2)	75.2(1)	174.2(1)	
O(1)–V(1)–O(3)		86.9(1)	
O(1)–V(1)–Cl(1)	87.6(1)		
O(1)–V(1)–C(13)	98.6(1)	92.5(1)	
O(2)–V(1)–O(3)		87.5(1)	
O(2)–V(1)–Cl(1)	86.4(1)		
O(2)–V(1)–C(13)	99.4(1)	93.2(1)	
O(3)–V(1)–C(13)		179.4(1)	
Cl(1)–V(1)–C(13)	172.4(1)		
cent(1) <sup>a</sup> –V(1)–cent(2)			145.9(1)
O(1)–K(1)–O(2)			90.1(2)
O(1)–K(1)–cent(3)			120.9(1)
O(1)–K(1)–cent(4)			110.7(1)
O(2)–K(1)–cent(3)			111.1(1)
O(2)–K(1)–cent(4)			115.6(1)
cent(3)–K(1)–cent(4)			108.0(1)

<sup>a</sup> Definitions: cent(1) represents the centroid of the plane of [C(8), C(9), C(10), C(11), C(13)]; cent(2) represents the centroid of the plane of [C(11'), C(12'), C(13')]; cent(3) represents the centroid of the plane of [C(1), C(2), C(3), C(4), N(1)]; cent(4) represents the centroid of the plane of [C(17), C(18), C(19), C(20), N(2)].

Accordingly, the last Fourier map yielded a reasonable position for the H atom connected to this particular carbon atom with angles and distance [V1···H13 = 2.50 Å; V(1)···H13–C13 = 80.1°] as expected for an agostic interaction.

The crystal structure of **2** (Figure 2) consists of a divalent vanadium center in a distorted octahedral environment defined by three meridionally arranged molecules of THF [V(1)–O(1) = 2.200(2) Å; V(1)–O(2) = 2.168(2) Å; V(1)–O(3) = 2.174(2) Å], two pyrrolide nitrogen atoms [V(1)–N(1) = 2.143(2) Å; V(1)–N(2) = 2.165(2) Å] and one carbon atom of the central phenyl ring [V(1)···C(13) = 2.615(1) Å]. As a result of the lower oxidation state of the central metal atom, all metal–ligand distances are longer than in **1**. The two deprotonated pyrrole rings of the ligand are coplanar with the metal center and with the two nitrogens trans to each other [N(1)–V(1)–N(2) = 176.1(1)°]. The

phenyl ring of the ligand is oriented in a way reminiscent of the  $\pi$ -coordination. However, all the V···C contacts are beyond the bonding range with the only exception of the carbon atom contained between the two pyrrolide attachments. However, as a result of the trans arrangement of the two N donor atoms, the phenyl ring shows considerably smaller slippage with a slightly smaller tilting [103.9°] with respect to the V···O(3) vector.

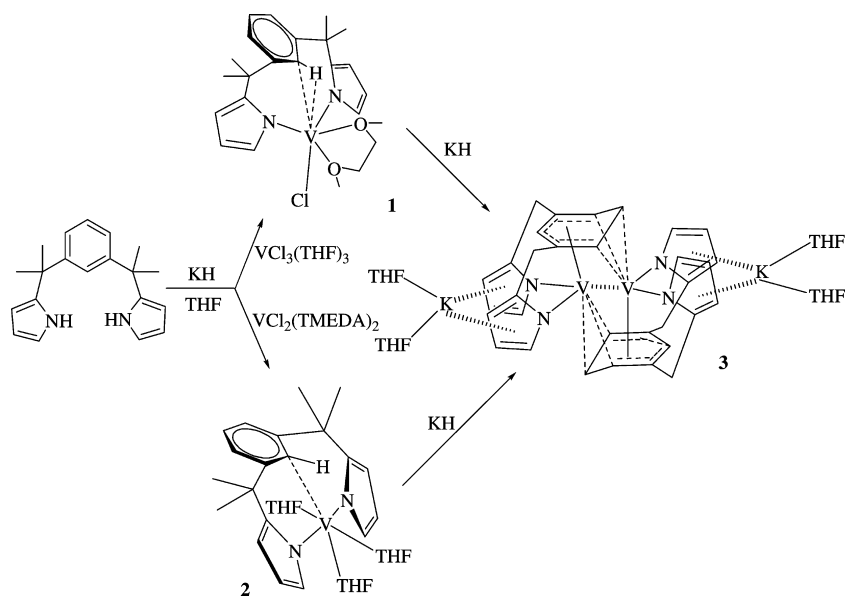
In striking contrast to the behavior of the closely related divalent complex of the tripyrrolyl ligand that gives the corresponding dinitrogen complex 2,5-[(2-pyrrolyl)(C<sub>6</sub>H<sub>5</sub>)<sub>2</sub>C]<sub>2</sub>(MeNC<sub>4</sub>H<sub>2</sub>)V]<sub>2</sub>( $\mu$ -N<sub>2</sub>) complex,<sup>7</sup> complex **2** is seemingly unreactive with dinitrogen. Although this behavior was not unexpected, given the presence of THF in the metal coordination sphere, attempts at extracting THF via treatment with Lewis acids, such as Me<sub>3</sub>Al, afforded only decomposition and formation of intractable materials. We have therefore attempted further reduction of the metal center to assess whether the ligand system could stabilize a monovalent vanadium and also to probe whether the aromaticity of the ring would be still resilient toward a strongly reducing V<sup>I</sup> center.

The reductions of both **1** and **2** proceeded smoothly with KH in THF to afford the corresponding dinuclear and diamagnetic [(THF)<sub>2</sub>K(1,3-bis-[(1'-pyrrol-2-yl)-1,1'-dimethyl)methyl]benzene)V]<sub>2</sub> (**3**) (Scheme 1). The NMR spectra were consistent with the proposed formulation as yielded by the crystal structure. The absence of CH<sub>2</sub> resonances in the DEPT–NMR experiments confirmed that no hydrogenation of the aromatic ring had occurred. The use of KH as reductant was advised by results recently obtained by us in dinitrogen chemistry where alkali hydrides often afforded slow and yet exceedingly clean and smooth reactions.<sup>7,34</sup> In only one instance did we observe partial N<sub>2</sub> hydrogenation.<sup>35</sup> The crystal structure of **3** (Figure 3) consists of a symmetry-generated dimer. Each vanadium atom is bonded to the ligand by using the two nitrogen atoms of the pyrrole rings [avg. V–N = 2.156 Å]. The central phenyl ring is also oriented with respect to vanadium in a fashion as expected for a  $\pi$ -interaction. Of the six ring carbon atoms, five are coplanar but only three reach a bonding contact with vanadium [V(1)–C(8) = 2.278(4) Å, V(1)–C(9) = 2.235(5) Å, V(1)–C(10) = 2.277(4) Å, V(1)–C(11) = 2.500(4) Å, V(1)–C(13) = 2.481(4) Å]. The remaining three carbon atoms identify a plane which gives a substantial folding to the ring (dihedral-angle between two planes is 28.5°). The short V–C distances with the second V atom provide an arrangement closely reminiscent of the  $\pi$ -allylic bonding [V(1')–C(11) = 2.424(5) Å, V(1')–C(12) = 2.097(5) Å, V(1')–C(13) = 2.415(4) Å]. Overall the coordination geometry around each vanadium atom may be described in terms of a trigonal bipyramid with the two N atoms and the second vanadium defining the equatorial plane and the centroid of one ring and the centroid of the allylic-type portion of the ring of

(34) Vidyaratne, I.; Scott, J.; Gambarotta, S.; Budzelaar, P. *Inorg. Chem.*, in press.

(35) Vidyaratne, I.; Scott, J.; Gambarotta, S.; Budzelaar, P. *Inorg. Chem.* **2007**, *46*, 7040.

Scheme 1



the other identical unit placed on the axis. Two potassium ions, each solvated by two molecules of THF, complete the structure by being  $\pi$ -coordinated to the two pyrrolide rings. The V–V distance [ $V(1)-V(1') = 2.412(1) \text{ \AA}$ ] falls in the range expected for a V–V multiple bond.<sup>9</sup>

There are two main features in the structure of **3**. The first is that the only bridging interaction is provided by the aromatic ring rather than by the nitrogen atoms of the pyrrolide groups. The second is the presence of a short V–V contact which, according to literature data,<sup>9</sup> might be in agreement with the presence of a V–V double or perhaps even triple bond. In any event, the diamagnetism of the complex indicates the presence of a strong coupling of the two vanadium centers, including at room temperature. The significant distortion<sup>36</sup> of the two aromatic rings indicates a disruption of ring aromaticity which in turn diagnoses a strong covalent bonding between the vanadium atom and the ring  $\pi$ -system. Dinuclear vanadium complexes where the bridging interaction is provided by one aromatic ring have been reported in the case of two  $V^{II}$  complexes: the diamagnetic  $(CpV)_2(\mu\text{-pentalene})^{9c}$  and  $(CpV)_2(\mu\text{-COT})^{9f}$ . In both cases, the existence of a triple bond between the vanadium centers has been proposed. However, both complexes exhibit temperature-dependent paramagnetism due to a Boltzmann population of the higher-energy, triplet electronic state with the nonzero magnetic moment. The V–V distances are remarkably different, 2.538 Å for  $(CpV)_2(\mu\text{-pentalene})$  and 2.44 Å  $(CpV)_2(\mu\text{-COT})$  which is only slightly longer than in **3**. This observation suggests that the V–V bond does not have a triple bond order in these ring-bridged dimers. To the best of our knowledge, complex **3** is the third

case of this type of complexes although two rings are used for bridging the two metal centers. The fact that complex **3** is diamagnetic suggests, together with the NMR results, that the dimeric structure is probably preserved in solution.

### Electronic Structures

**Complexes 1 and 2.** The structures from the spin-unrestricted B3LYP/TZVP calculations present geometrical parameters in reasonable agreement with the crystallographic values (Figures 4 and 5). Complexes **1** and **2** have the high-spin electronic configurations (the spin triplet and quartet, respectively) consistent with the observed magnetic moments of the two species. In both cases, two and three, predominantly metal  $t_{2g}$ -based, and nearly degenerate orbitals are singly occupied. As a result, the NPA-derived spin density of the V atom is 2.08 and 2.94 in complexes **1** and **2**, respectively. In complex **1**, the valence index of the V atom is 5.27, and the NPA-derived atomic charge of the central atom (1.25 au) indicates a very significant covalent contribution to the metal–ligand bonding. The ligand-to-metal charge donation is 0.42  $e^-$  for  $Cl^-$ , 0.24  $e^-$  for DME, and 1.09  $e^-$  for the ligand. Both the 3d and 4s orbitals of the metal atom participate in these interactions with 0.21  $e^-$  transferred to the 4s orbital and 1.49  $e^-$  accepted by the unoccupied 3d orbitals. The resulting metal–ligand bond orders<sup>27</sup> are 0.73–0.76 for the V– $N_L$  bonds, 0.91 for the V–Cl bond, and 0.18–0.22 for the V– $O_{DME}$  bonds. Such significant metal–ligand covalency is reflected in the short metal–ligand bond distances (Figures 4 and 5) and in the spin polarization for the  $N_L$  atoms which each carry a spin density of  $-0.05$ .

In complex **2**, the covalent contribution to the metal–ligand bonding is reduced, and the valence index and NPA-derived atomic charge of the V atom are 4.15 and 1.27 au, respectively. The ligand-to-metal charge donation is 0.28  $e^-$  for the three THF ligands and 0.45  $e^-$  for L. The resulting metal–ligand bond orders are 0.31–0.32 for the V– $N_L$  bonds and 0.10–0.13 for the V– $O_{THF}$  bonds.

(36) (a) For examples of distorted coordinated or partly hydrogenated phenyl rings, see Bruck, M. A.; Copenhaver, A. S.; Wigley, D. E. *J. Am. Chem. Soc.* **1987**, *109*, 6525. (b) Steffey, B. D.; Chesnut, R. W.; Kerschner, J. L.; Pellechia, P. J.; Fanwick, P. E.; Rothwell, I. P. *J. Am. Chem. Soc.* **1989**, *111*, 378. (c) Steffey, B. D.; Rothwell, I. P. *J. Chem. Soc., Chem. Commun.* **1990**, 213. (and references therein). (d) Aharonian, G.; Gambarotta, S.; Yap, G. P. A. *Organometallics* **2002**, *21*, 4257.



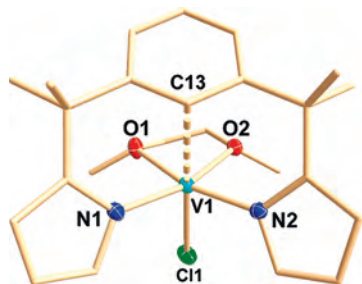


**Figure 1.** Simplified drawing of **1** with selected atoms drawn at the 30% probability level.

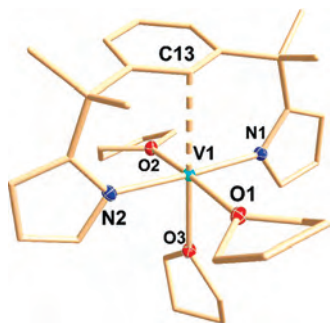


**Figure 2.** Crystal structure of **2** with selected atoms drawn at the 30% probability level. The hydrogen atoms are not shown.

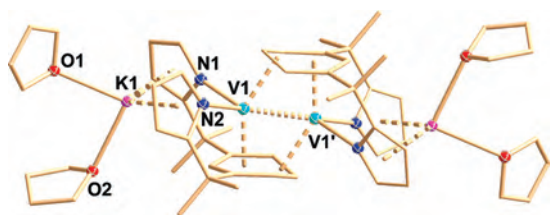


**Figure 3.** Crystal structure of **3** with selected atoms drawn at the 50% probability level. The hydrogen atoms are not shown.

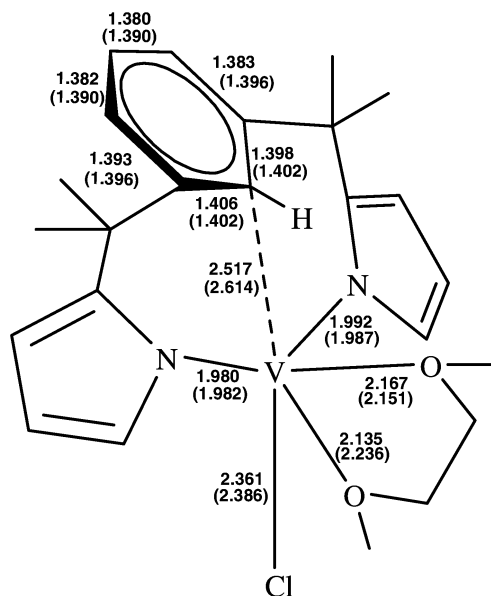


**Figure 4.** Relevant experimental and B3LYP/TZVP-calculated (in parenthesis) bond distances for **1**.

In both cases, the inclination of the phenyl ring toward the vanadium atom, as discussed above, might suggest the presence of an agostic interaction. This interaction is expected to elongate the corresponding C–H bond, and the resulting

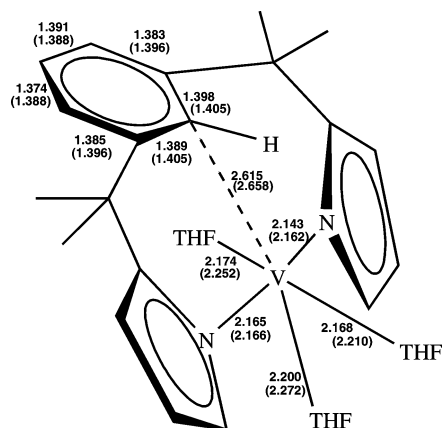


**Figure 5.** Relevant experimental and B3LYP/TZVP-calculated (in parenthesis) bond distances for **2**.

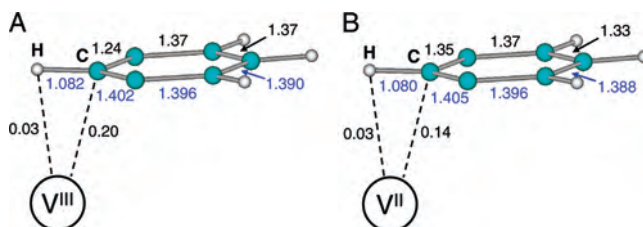


**Figure 6.** Calculated Mayer bond orders and interatomic distances (Å, shown in blue) for complexes **1** (A) and **2** (B) at the B3LYP/TZVP level. Only relevant atoms are shown.

three-center M–C–H bond order  $B_{MCH}$  is expected to be positive (reaching  $B_{MCH}$  of  $\sim 0.296$  for a full 2-electron 3-center bond). The DFT calculations revealed instead that the two-center V–H interaction and the three-center V–C–H interaction are negligible in both species. The calculated C–H distance is unperturbed (Figure 6), and the V–H distances in complexes **1** and **2** are 2.68 Å and 2.66 Å, respectively, and are too long to impart a significant agostic character to the interaction between the occupied  $\sigma_{C-H}$  orbital and the vanadium acceptor orbitals. A substantial interaction was found between the V and C atoms through a charge transfer from the occupied  $\pi$ -orbital of the central phenyl ring of L into the  $3d_z^2$  and  $4s$  orbitals of vanadium. This interaction results in a Mayer bond order  $B_{V-C}$  of 0.20 in complex **1** (with the 0.14 and 0.06 contributions of the  $3d_z^2$  and  $4s$  orbitals, respectively) and 0.14 in complex **2**. However, the V–C coupling only weakly perturbs the conjugation of the  $\pi$ -system (for example, the C–C bond orders in the ring are 1.24, 1.37, and 1.37 in complex **1**, Figure 6A) and does not disrupt the planarity of the phenyl ring.

**Complex 3.** There are two main features in the description of the electronic structure of **3**. The first is the V–V bonding while the second arises from the complex metal–ring interaction. At first glance, the short V–V distance, together with the observed diamagnetism, could be interpreted as an indication of the presence of a V–V multiple bond. However, our DFT calculations suggest that only a weaker covalent interaction exists between the two metal centers in spite of the short  $V\cdots V$  contact, with a Mayer bond order  $B_{V-V}$  of  $\sim 1.5$  (Table 3 and Figure 8). The reliability of the calculation is indicated by the reasonable agreement between the values

**Table 3.** Electronic Energy, V–V Distance, and Mayer Bond Order for the Lowest-Energy Singlet, Triplet, Pentet, and Septet States of **3** and (CpV)<sub>2</sub>(μ-pentalene) from the PBE Calculations

	<b>3</b>			(CpV) <sub>2</sub> (μ-pentalene)		
	$\Delta E^a$ (kcal mol <sup>-1</sup> )	$d_{V-V}$ (Å)	$B_{V-V}$	$\Delta E^a$ (kcal mol <sup>-1</sup> )	$d_{V-V}$ (Å)	$B_{V-V}$
CS singlet	0.1	2.387	1.51	12.3	2.375	1.92
OS singlet	0.0	2.395	1.45	0.0	2.568	0.95
triplet	13.5	2.521	0.89	5.3	2.499	1.24
pentet	19.0	2.758	0.54	13.2	2.788	0.87
septet				12.4	3.140	0.26

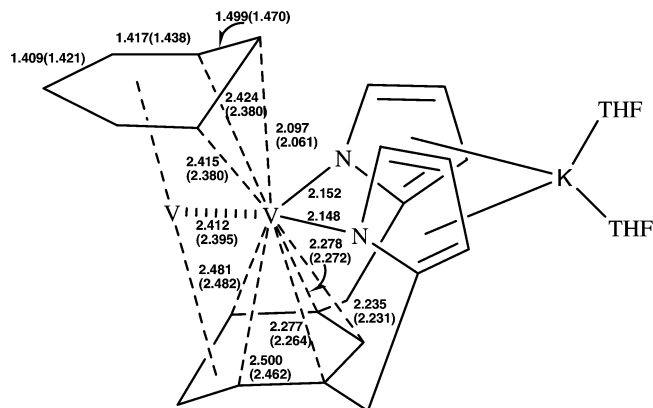
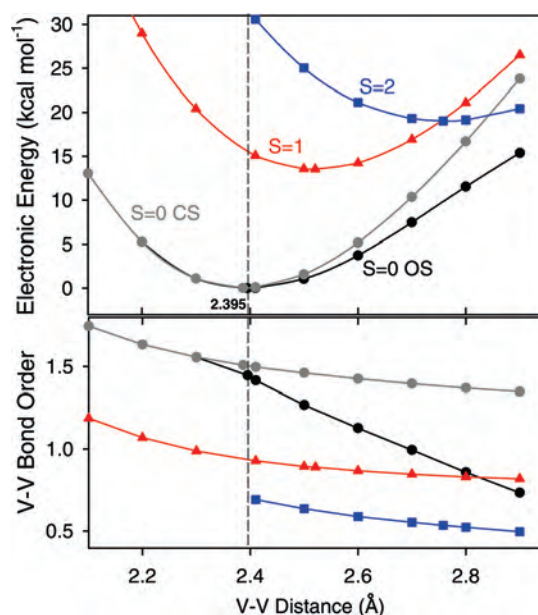
<sup>a</sup> Relative the electronic energy of the singlet ground-state.

of the calculated and crystallographic geometry parameters (Figure 7).

By using the spin-unrestricted PBE calculations, we have calculated both the V–V bond order and the electronic energy as a function of the V–V distance for the following electronic configurations: (a) open-shell (OS) singlet with 2 unpaired electrons on each V center antiferromagnetically coupled to those of the other metal center, (b) closed-shell (CS) with all electrons paired, (c) spin-triplet state, and (d) spin-pentet state (Figure 8). The nature of the singlet ground-state changes from the CS electronic configuration (at the V–V distances less than 2.3 Å) to the OS electronic configuration. The potential energy surfaces (PES) also show that both triplet and pentet states are well above the singlet ground-state in the 2.1–2.7 Å V–V distance range. At very long V–V distances, the OS singlet and pentet state become degenerate because of the loss of the V–V interaction. In all cases, the PES curves are fairly shallow; thus, this suggests that the V–V interactions are indeed weak similarly to the behavior of the Cr–Cr quadruple bonds.<sup>10</sup> The PBE calculations correctly predicted the minimum of energy at the experimental value of the V–V distance. As the V–V bond elongates, the V–V bond order decreases from 1.45 at the energy minimum to 0.73 at 2.9 Å (Figure 8).

The triplet and pentet states show the PES minima at longer distances and at weaker covalent interactions between the two V atoms (Table 3 and Figure 8). Incidentally, this takes us to the striking similarity between this species and the other two dinuclear complexes reported previously of the V(II) nearly-diamagnetic dimers bridged by a π-system for which a description featuring a V–V triple bond was proposed.<sup>9c,f</sup> To account for the short V–V distances, a closed-shell singlet configuration was assumed in both cases. Our DFT calculations at the BPE/TZVP level for the pentalene-bridged structure,<sup>9c</sup> also with the input of an OS singlet wave function, gave a good match of the calculated (2.568 Å, Table 3) and the crystallographic (2.54 Å) V–V distances. In contrast, the geometry optimization of the CS singlet generates a structure that is higher in energy and has the V–V distance of 2.375 Å which is too short relative to the crystallographic value.

Different from the case of **3**, the DFT calculations show that there is a substantial energy gap between the CS and OS singlet states and that the OS singlet is the true ground electronic state even at very short V–V distances (Figure 9). Furthermore, the close proximity with the triplet state,

**Figure 7.** Relevant experimental and calculated in parenthesis bond distances for **3**.**Figure 8.** Potential energy profiles and bond order profiles calculated for the open-shell singlet (black), closed-shell singlet (gray), triplet (red), and pentet (blue) electronic configurations of **3**. The vertical dash line indicates the position of the ground-state energy minimum.

with the electronic energy of 5.3 kcal mol<sup>-1</sup> (Table 3), nicely accounts for the experimentally observed residual paramagnetism and thermal dependence. These observations confirm that in these two π-system bridged dimers the V–V interaction is consistently weak in what can normally be regarded as a V–V single bond (the V–V bond order for the OC singlet energy minimum is 0.95). The bonding within the complex is indeed dominated by the vanadium–ligand interaction. On the basis of these calculations and available spectroscopic evidence, we suggest that the OS singlet with the antiferromagnetic coupling of the unpaired d electrons on each V is the most realistic description of the electronic configuration of these π-bonded dimers.

The bonding of vanadium with the two distorted phenyl rings in complex **3** is of interest. The overall bond order between vanadium and each ring is about 1.40–1.45 (Figure 10). The large ring distortion is the result of the interaction with both metal centers. The bonding may be described in terms of two separate processes. The charge transfer from vanadium to the ring is obtained by engaging a ligand π\*



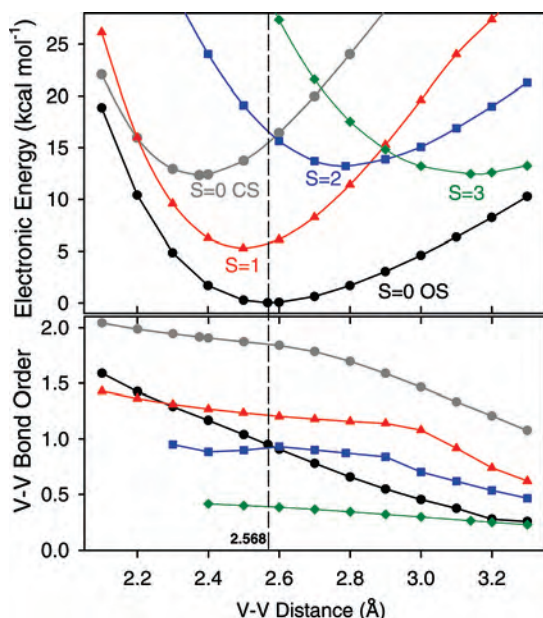


**Figure 9.** Potential energy profiles and bond order profiles calculated for the open-shell singlet (black), closed-shell singlet (gray), triplet (red), pentet (blue), and septet (green) electronic configurations of  $(\text{CpV})_2(\mu\text{-pentalene})$ . The vertical dashed line indicates the position of the ground-state energy minimum.

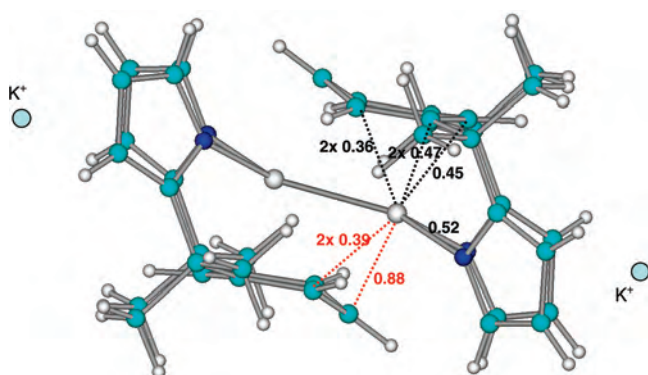


**Figure 10.** Mayer bond orders for metal–ligand bonds for the ground electronic state of complex **3**.

empty orbital which accounts for a transfer of total charge density of about one electron. The second portion, which protrudes out of plane, has the  $\pi$ -system completely obliterated by the back-donation into the second vanadium center. In the process, the V–C bonds with a definite  $\sigma$ -character are formed accounting for an overall V–C bond order of about 2.10 and 1.66 for the first and second ligands (Figure 10). There is therefore an interesting synergistic effect within

the dimeric unit in terms of back-donation from one metal into a portion of one ring, donation from the other ring portion into the second metal, and vice versa for the second ring. Overall, the aromatic ring carries a near to zero charge in spite of the perturbation of the  $\pi$ -system. From this point of view, the bonding to vanadium does not necessarily imply an increase of the vanadium oxidation state. Indeed, the vanadium atom can realistically be regarded as  $d^4 \text{V(I)}$ .

The effect of the potassium cations coordinated to the periphery of the structure appears to be purely electrostatic. The NPA-derived charge of the potassium atoms in **3** is +0.96 au. Removal of the counter-cations did not change the description of the electronic structure of the vanadium dimer. The bonding description remained essentially the same.

In conclusion, we have characterized three new low-valent vanadium complexes of a  $\sigma$ - and  $\pi$ -donor ligand system. Complex **3** provides a rare example of a vanadium dimer with two bridging  $\pi$ -systems and a short V–V distance. In line with the behavior of quadruply bonded  $d^4 \text{Cr(II)}$  systems, the V–V interaction is rather weak, which by decreasing stability and improving reactivity opens an interesting perspective for the purpose of electron storage and preparation of highly reactive vanadium(I) synthons. The apparent non-ability of this system to interact with dinitrogen is likely caused by strong covalent interactions of the vanadium atom with the  $\pi$ -system of the central aromatic ring. It is worth reminding that the replacement of the central phenyl ring with *N*-MePyrrole enabled both dinitrogen fixation and cleavage.<sup>7b</sup> Thus, the metal interaction with the aromatic ring is preferential to that with  $\text{N}_2$ . The lowering of the oxidation state, expected to increase the reactivity of the metal center, resulted in a direct V–V weak bonding interaction mainly promoted by the complex interaction with the aromatic ring.

**Acknowledgment.** This work was supported by the Natural Science and Engineering Council of Canada (NSERC). We thank Professor Tom K. Woo (U. Ottawa) for use of the computing facilities, funded by the Canada Foundation for Innovation, and the Ontario Research Fund.

**Supporting Information Available:** Complete crystallographic data (CIF) and DFT-optimized atomic coordinates for the complexes reported in this paper (PDF). This material is available free of charge via the Internet at <http://pubs.acs.org>.

IC702280G